Available online at www.sciencedirect.com
ScienceDirect
Bioelectrochemistry 70 (2007) 435–439
Bioelectrochemistry
www.elsevier.com/locate/bioelechem

Electrochemical behaviors of native and thermally denatured fish DNA in the presence of cytosine derivatives and porphyrin by cyclic voltammetry using boron-doped diamond electrode

Amara Apilux [a], Masaaki Tabata [a,*], Orawon Chailapakul [b]

[a] Department of Chemistry, Faculty of Science and Engineering, Saga University, 1 Honjo-machi, Saga 840-8502, Japan
[b] Department of Chemistry, Faculty of Science, Chulalongkorn University, 254 Phyathai Road, Patumwan, Bangkok 10330, Thailand

Received 27 December 2005; accepted 4 July 2006
Available online 6 July 2006

Abstract

The electrochemical behaviors of native and thermally denatured fish DNA was investigated using boron-doped diamond (BDD) film electrode by cyclic voltammetry. The BDD electrode afforded us to measure weak current less than μA for the DNA solution in 100 μl. The mixture of acetic acid and sodium acetate solution (0.2 M) was used as a supporting electrolyte. Two oxidation peaks were observed at about +1.1 V and +1.3 V at pH 4.6 for thermally denatured fish DNA. This is due to the oxidation of guanine and adenine in the denatured fish DNA, respectively. In contrast, the native fish DNA showed ill-defined peaks at +1.1 V. Furthermore, the electrochemical behaviors of thermally denatured fish DNA were studied in the presence of cytosine, cytidine, cytidine-5-monophosphate, tetrakis(1-methypyridinium-4-yl)porphyrin (H_2(TMPyP)$^{4+}$) and Ru^{II}(TMPyP)$^{4+}$. The oxidation peak intensity at +1.1 V gradually decreased with the increase of the concentrations of the above compounds. Based on the above studies, electrochemical behaviors of the thermally denatured fish DNA at BDD electrode is discussed.

Keywords: Cyclic voltammetry; Boron doped diamond electrode; Denatured DNA

1. Introduction

During the last decades, much interest has been paid on the studies of carcinogenic or mutagenic effects of chemicals or metal ions which are usually used in laboratory of chemistry or biology and also some aspects in industries [1–7]. DNA is easily oxidatively cleaved or damaged in the presence of oxidants like H_2O_2 and metal ions through the generation of endogenous reactive radicals [8–11]. In our previous papers [12], we have found selective DNA cleavage in the presence of Good's buffers and gold(III) through the formation of nitrogen centered radicals. The cleavage has been ascribed to the oxidation of guanine moiety of DNA. In order to confirm the oxidation process of DNA, we investigated the electrochemical behaviors of DNA.

DNA is an electroactive species producing reduction and oxidation signals in various polarography and voltammetry modes. The reduction of DNA has been observed at mercury electrodes, whereas the oxidation at solid electrodes, such as glassy carbon (GC), graphite, gold and etc. [13–16]. Since these methods are very easy to operate, fast and inexpensive, therefore DNA has been intensively studied using electrochemical methods for many years.

Recently, the boron-doped diamond (BDD) film electrode has been used as a unique electrode material for electroanalysis because of its attractive properties, such as large electrochemical window in aqueous solution, low background current and high anodic stability of measurement [17].

In this work, we studied the electrochemical behaviors of thermally denatured fish DNA using the BDD electrode in the presence of cytosine derivatives and tetrakis(1-methypyridinium-4-yl)porphyrin H_2(TMPyP)$^{4+}$ and Ru^{II}(TMPyP)$^{4+}$, and the electrochemical behavior of thermally denatured fish DNA is discussed.

* Corresponding author. Tel./fax: +81 952 28 8560.
E-mail address: tabatam@cc.saga-u.ac.jp (M. Tabata).

1567-5394/$ - see front matter © 2006 Published by Elsevier B.V.
doi:10.1016/j.bioelechem.2006.07.001

2. Experimental

2.1. Instrumentation

Cyclic voltammetry (CV) measurements were performed by using an 802A Electrochemical Analyzer (CH Instruments) at the following settings: initial potential = −0.5 V and final potential = 1.5 V. The scan rate was 10 mV/s. The three electrodes system consisted of a boron doped diamond (BDD) thin film electrode as a working electrode, Ag|AgCl|3M NaCl as a reference electrode and a stainless steel tube as an auxiliary electrode and a micro flow cell (BAS INC.). UV–Vis spectra were obtained from a Shimadzu UV 2100 spectrophotometer. The base pairs concentration of DNA was determined by absorbance measurement at the absorption maximum of 260 nm. Circular dichroism (CD) spectra of DNA were recorded on a Jasco J-700 spectropolarimeter (Japan).

2.2. Chemicals and reagents

All chemicals were analytical grade. All solutions were prepared by using double distilled water. Cytosine, cytidine and cytidine-5-monophosphate disodiumsalt were purchased from TCI (Japan). Tetrakis(1-methypyridinium-4-yl)porphyrin, $H_2(TMPyP)^{4+}$, was purchased from Dojindo Laboratories (Japan) as tosylate and $Ru^{II}(TMPyP)^{4+}$ was synthesized in our laboratory. Acetate buffer solutions were prepared from sodium acetate (Wako) and acetic acid (Wako), and pH was adjusted with sodium hydroxide and acetic acid. The pH value of each solution was measured before use.

2.3. Preparation of DNA solution

DNA stock solutions were prepared by dissolving sodium salt of deoxyribonucleic acid extracted from salmon spermary, Wako (Japan) in double distilled water. DNA concentration was determined by the measurement of absorbance at 260 nm. Then the stock solution was diluted to the appropriate concentration by the addition of acetate buffer solution (pH 4.6) before use.

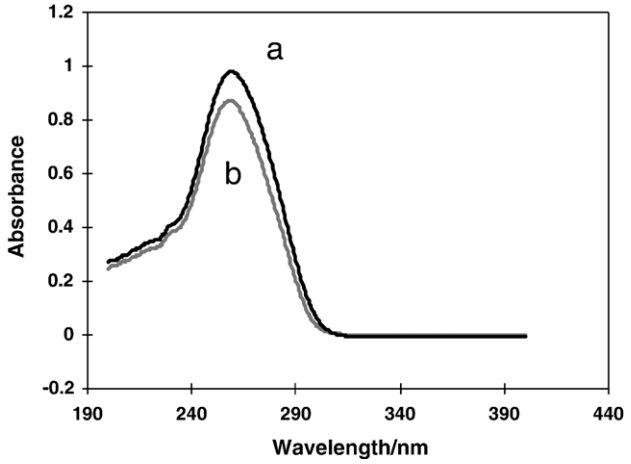

Fig. 1. UV spectra of the thermally denatured fish DNA (a) and the native fish DNA (b) in 0.2 M acetate buffer pH 4.6.

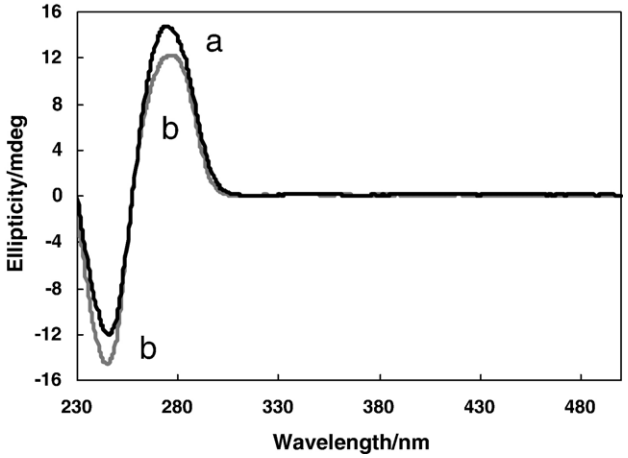

Fig. 2. CD spectra of the thermally denatured fish DNA (a) and the native fish DNA (b) in 0.2 M acetate buffer pH 7.6.

Thermally denatured DNA was prepared by heating it at 95 °C for 15 min and then cooled rapidly in an ice-bath.

3. Results and discussion

3.1. UV and CD spectra of fish DNA

Fig. 1 shows the UV spectra of the native and thermally denatured fish DNA. It shows that the absorbance at 260 nm is higher for the denatured fish DNA than the native fish DNA. CD spectrum was measured at pH value from 3 to 12. As can be seen in Fig. 2, the spectrum of the native fish DNA and the thermally denatured fish DNA showed a positive and a negative peak at 270 nm and 243 nm, respectively. The intensity of the positive peak at 270 nm increased and that of negative peak at 243 nm decreased when native fish DNA was denatured as observed before [15]. The results of UV and CD spectra indicate that the structure of the fish DNA was changed by temperature denaturalization.

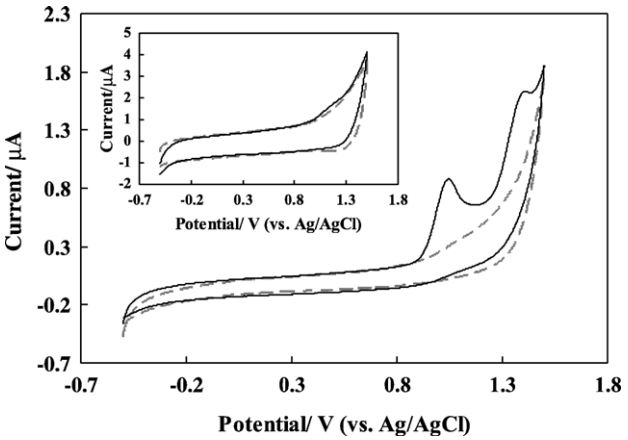

Fig. 3. Cyclic voltammograms of 1 mM in bp of the thermally denatured fish DNA in 0.2 M acetate buffer pH 4.6 at BDD electrode at scan rate 0.01 Vs^{-1}. Inset: 1 mM in bp the native fish DNA in 0.2 M acetate buffer pH 4.6 at BDD electrode at scan rate 0.01 Vs^{-1}. The background cyclic voltammograms are also shown (dash line).

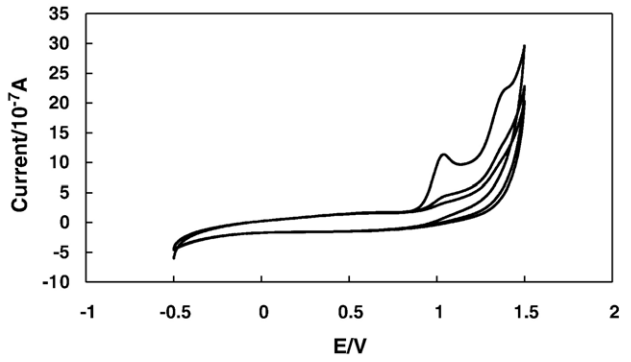

Fig. 4. Cyclic voltammograms (vs. Ag/AgCl) of 1 mM in bp of thermally denatured fish DNA in 0.2 M acetate buffer pH 4.6 at BDD electrode at scan rate 0.01 Vs^{-1} for three successive scans.

3.2. Cyclic voltammetry of fish DNA

The cyclic voltammograms for the native and thermally denatured fish DNA in 0.2 M CH_3COOH–CH_3COONa buffer (pH 4.6) at the BDD electrode are shown in Fig. 3. As shown in the inset of Fig. 3, the BDD electrode provided a stable background and ill-defined oxidation peak of the native fish DNA at the potential ~1.1 V vs. Ag/AgCl. Whereas, the cyclic voltammogram of the thermally denatured fish DNA showed two clear peaks at the potential ~1.1 V and ~1.3 V vs. Ag/AgCl. The peaks are due to the oxidation of guanine and adenine residues, respectively [15]. Upon the denaturation of DNA, double stranded DNA macromolecules separate partly into two single stranded DNA by the rupture of hydrogen bonds, so free guanine and adenine are produced. It means that, guanine and adenine base residues are exposed to electrode surface when the fish DNA is denatured, so the oxidative reaction easily occurs. The primary oxidation sites of guanine and adenine structures are carbon atoms at 8 and 2 positions of guanine and adenine of DNA bases, respectively. In contrast, an ill-defined peak for the native fish DNA as shown in inset of Fig. 3 indicates the difficulty of oxidation.

Fig. 4 shows a successive cyclic voltammogram of the thermally denatured fish DNA. The two signals decreased in the second and the third cycle due to the adsorption of the denatured fish DNA which forms a DNA multilayer on the BDD electrode surface.

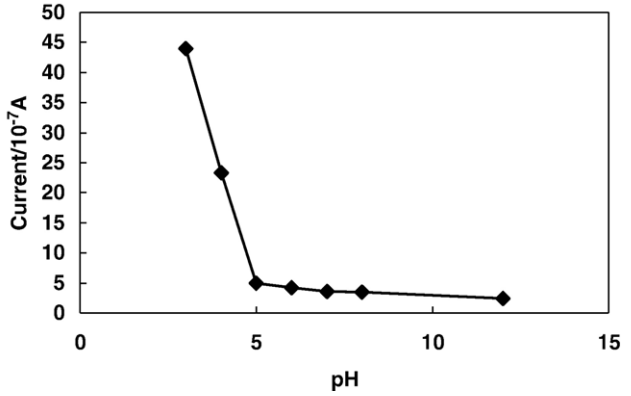

Fig. 5. The effect of pH on oxidation peak current of guanine at scan rate 0.01 Vs^{-1}.

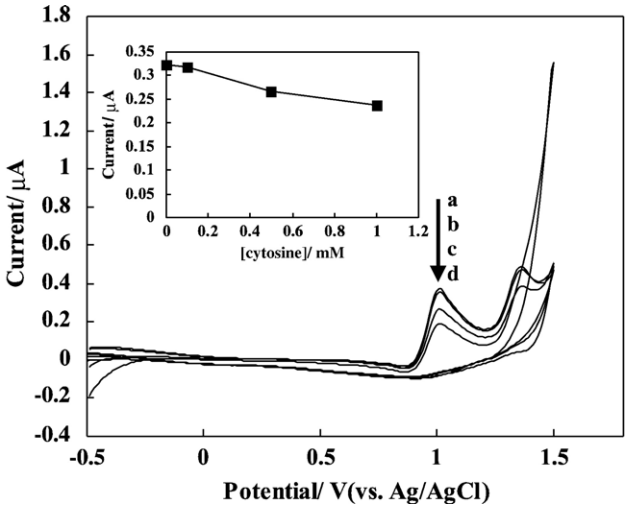

Fig. 6. Baseline subtracted cyclic voltammograms (vs. Ag/AgCl) of 5.0×10^{-4} M in bp of the denatured fish DNA in the presence of cytosine: (a) 0 M; (b) 1.0×10^{-4} M; (c) 5.0×10^{-4} M; (d) 1.0×10^{-3} M, respectively in 0.2 M acetate buffer pH 4.6 at BDD electrode at scan rate 0.01 Vs^{-1}. Inset: plot of peak currents vs. cytosine concentrations at ~1.1 V.

The effect of pH on CV was investigated from pH 3 to 12. For the temperature denatured fish DNA, it was found that the guanine peak at +1.1 V shifted to low potential and its intensity decreased when the pH increased (Fig. 5). A peak of the oxidized adenine was also observed at +1.3 V at pH 4.5–5.0. The nitrogen atoms of cytosine and thymine are protonated at pH lower than 5 that prevents the hydrogen bonding formation with guanine and adenine to reform DNA after the denaturation of DNA. The hydrogen-bond breaking enhances the denature of DNA. In contrast, the native fish DNA showed only ill-defined peak at low pHs.

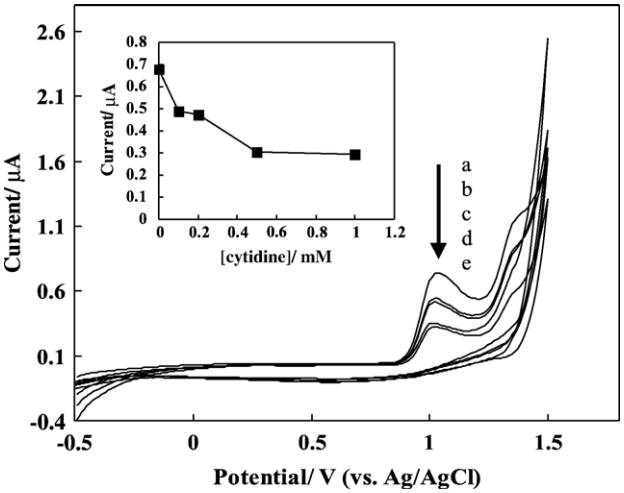

Fig. 7. Baseline subtracted cyclic voltammograms (vs. Ag/AgCl) of 7.5×10^{-4} M in bp of the denatured fish DNA in the presence of cytidine: (a) 0 M; (b) 1.0×10^{-4} M; (c) 2.0×10^{-4} M; (d) 5.0×10^{-4} M and (e) 1.0×10^{-3} M, respectively in 0.2 M acetate buffer pH 4.6 at BDD electrode at scan rate 0.01 Vs^{-1}. Inset: plot of peak current vs. cytidine concentration at ~1.1 V.

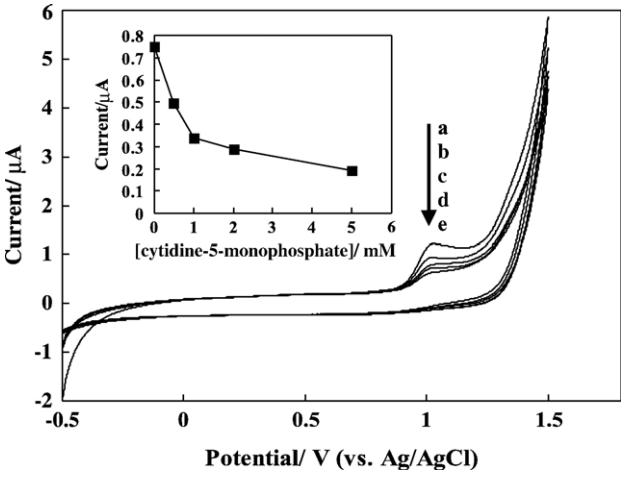

Fig. 8. Cyclic voltammograms (vs. Ag/AgCl) of 7.5×10^{-4} M in bp of the denatured fish DNA in the presence of the cytidine-5-monophosphate: (a) 0 M; (b) 5.0×10^{-4} M; (c) 1.0×10^{-3} M; (d) 2.0×10^{-3} M and (e) 5.0×10^{-3} M, respectively in 0.2 M acetate buffer pH 4.6 at BDD electrode at scan rate 0.01 Vs^{-1}. Inset: plot of the peak current vs. cytidine-5-monophosphate concentration at ~1.1 V.

3.3. Cyclic voltammetry for the interaction of cytosine, cytidine and cytidine-5-monophosphate with thermally denatured fish DNA

The cyclic voltammetry of cytosine, cytidine and cytidine-5-monophosphate in acetate buffer pH 4.6 did not show any oxidation peaks at BDD electrode.

The cyclic voltammograms of the thermally denatured fish DNA in the presence of cytosine, cytidine and cytidine-5-monophosphate in acetate buffer pH 4.6 were shown at Figs. 6, 7 and 8, respectively. The guanine peak at potential 1.05 V decreased with the addition of cytosine. This indicates that cytosine interacts with the denatured fish DNA through a hydrogen-bonding with guanine. Hence, it is difficult to denature

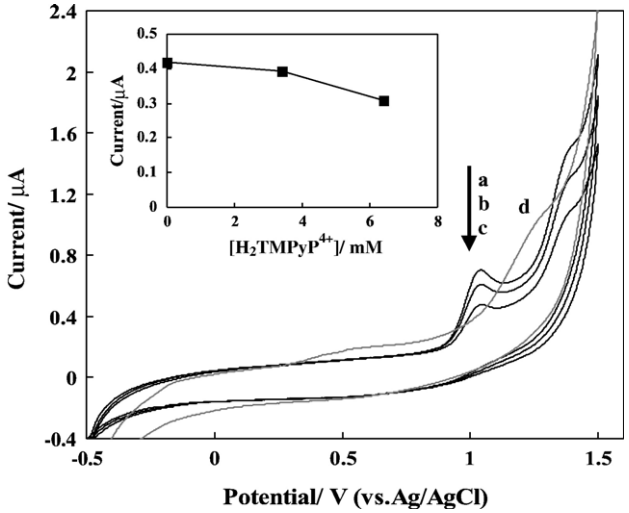

Fig. 9. Cyclic voltammograms (vs. Ag/AgCl) of: 7.5×10^{-4} M in bp of denatured fish DNA in 0.2 M acetate buffer at pH 4.6 at the concentrations of $H_2(TMPyP)^{4+}$; (a) 0 M, (b) 3.4×10^{-6} M and (c) 6.4×10^{-6} M, (d) 1.0×10^{-5} M $H_2(TMPyP)^{4+}$ in the absence of the denatured fish DNA, at BDD electrode at scan rate 0.01 Vs^{-1}. Inset: plot of peak current vs. $H_2(TMPyP)^{4+}$ concentration at ~1.1 V.

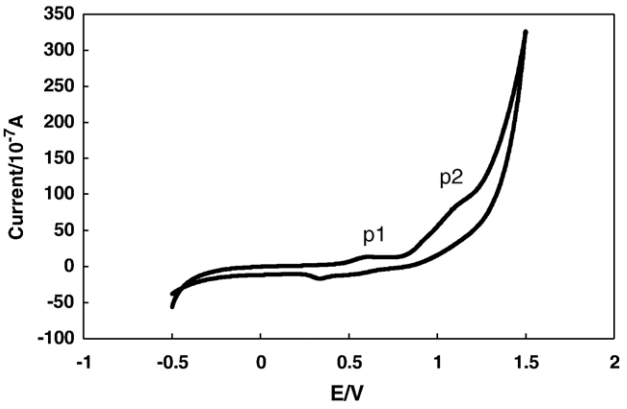

Fig. 10. Cyclic voltammogram (Ag/AgCl) of 2.4×10^{-4} M RuII$(TMPyP)^{4+}$ in 0.2 M acetate buffer at pH 4.6 at BDD electrode at scan rate 0.01 Vs^{-1}.

fish DNA. As the result, the electrochemical behavior of the denatured fish DNA decreased on BDD electrode. Similar results were observed for the addition of cytidine and cytidine-5-monophosphate. Furthermore, the cytidine-5-monophosphate showed the largest decrease in CV peak at the potential ~1.1 and ~1.3 V vs. Ag/AgCl.

3.4. Cyclic voltammetry for the interaction of porphyrin with thermally denatured fish DNA

The interaction of $H_2(TMPyP)^{4+}$ and $Ru^{II}(TMPyP)^{4+}$ with the thermally denatured fish DNA was studied. When $H_2(TMPyP)^{4+}$ was mixed in the denatured fish DNA, we found that the oxidation peak of the denatured fish DNA at potential about 1.1 V decreased, as shown in Fig. 9. Because positively charged $H_2(TMPyP)^{4+}$ combines with phosphate groups of DNA and/or intercalate into DNA bases [7]. As the result, electrochemical behavior of the denatured fish DNA decreased at BDD electrode. Fig. 9.d shows a broad peak of $H_2(TMPyP)^{4+}$ at potential ~1.2 V. The oxidation of $H_2(TMPyP)^{4+}$ also was suppressed by the binding to DNA.

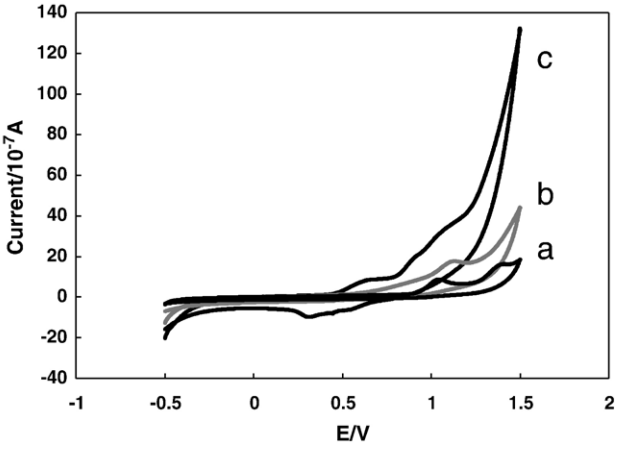

Fig. 11. Cyclic voltammograms (vs. Ag/AgCl) of 1.0×10^{-3} M in bp of the denatured fish DNA in 0.2 M acetate buffer at pH 4.6 at the concentrations of $Ru^{II}(TMPyP)^{4+}$: (a) 0 M; (b) 1.2×10^{-4} M and (c) 2.4×10^{-4} M, at BDD electrode at scan rate 0.01 Vs^{-1}. Inset: plot of the peak current vs. $Ru^{II}(TMPyP)^{4+}$ concentration at ~1.1 V.

$Ru^{II}(TMPyP)^{4+}$ showed oxidation peaks at potential 0.6 V and 1.2 V and reduction peak at potential 0.3 V in the absence of DNA as shown in Fig. 10. Fig. 11 shows cyclic voltammogram of $Ru^{II}(TMPyP)^{4+}$ in the presence of the denatured DNA of 1×10^{-3} M in base pair. The oxidation peaks of the denatured DNA gradually decrease with increased $Ru^{II}(TMPyP)^{4+}$. Due to the interaction of $Ru^{II}(TMPyP)^{4+}$ with the denatured fish DNA, it is difficult for the denatured fish DNA-$Ru^{II}(TMPyP)^{4+}$ complex to be oxidized at BDD electrode.

4. Conclusion

The thermally denatured fish DNA is electrochemical active in 0.2 M acetate buffer pH 4.6 at BDD electrode and the oxidation of guanine and adenine were detected. The oxidation of the denatured DNA were observed at pH lower than 5 and suppressed in the presence of cytosine, cytidine, cytidine-5-monophosphate, $H_2(TMPyP)^{4+}$ and $Ru^{II}(TMPyP)^{4+}$. The cytosine derivatives stabilized the denatured DNA through a hydrogen-bonding with guanine and prevented from the oxidation of DNA. Similarly, the cationic porphyrins also stabilized the denatured DNA structure through intercalation and ionic interaction with DNA. BDD electrode affords us to detect electrochemical behaviors of thermally denatured DNA by cyclic voltammetry due to its low background current.

Acknowledgements

This work was supported in part by a PSJP (Postgraduate Special Joint Program) scholarship (A. Amara) and Grants-in-Aid, for Exploratory (No. 176534) (M. Tabata), from the Ministry of Education, Science, Technology, Sports and Culture of Japan.

References

[1] S. Kawanishi, Y. Hiraku, M. Murata, S. Oikawa, The role of metals in site-specific DNA damage with reference to carcinogenesis, Free Radic. Biol. Med. 32 (2002) 822–832.
[2] S. Kawanishi, D. Inoue, S. Sano, Mechanism of DNA cleavage induced by sodium chromate(VI) in the presence of hydrogen peroxide, J. Biol. Chem. 261 (1986) 5952–5958.
[3] K. Hirakawa, K. Midorikawa, S. Oikawa, S. Kawanishi, Carcinogenic semicarbazide induces sequence-specific DNA damage through the generation of reactive oxygen species and the derived organic radicals, Mutat. Res. 536 (2003) 91–101.
[4] M. Murata, A. Tamura, M. Tada, S. Kawanishi, Mechanism of oxidative DNA damage induced by carcinogenic 4-aminobiphenyl, Free Radic. Biol. Med. 30 (2001) 765–773.
[5] IARC Working Group, 4-Aminobiphenyl, in: IARC (Ed.), IARC Monographs on the Evaluation of the Carcinogenic Risk of Chemicals to Man, vol. 1, IARC, Lyon, 1972, pp. 74–79.
[6] IARC Working Group, Tobacco habits other smoking; betelquid and areca nut chewing; and some related nitrosamines, in: IARC (Ed.), IARC Monographs on the Evaluation of the Carcinogenic Risk of Chemicals to Man, vol. 38, IARC, Lyon, 1985, p. 392.
[7] M. Murata, S. Kawanishi, Oxidative DNA damage by vitamin A and its derivative via superoxide generation, J. Biol. Chem. 275 (2000) 2003–2008.
[8] S. Inoue, S. Kawanishi, Hydroxyl radical production and human DNA damage induced by ferric nitrilotriacetate and hydrogen peroxide, Cancer Res. 47 (1987) 6522–6527.
[9] K. Yamamoto, S. Inoue, A. Yamazaki, T. Yoshinaga, S. Kawanishi, Site-specific DNA damage induced by cobalt(II) ion and hydrogen peroxide: role of singlet oxygen, Chem. Res. Toxicol. 2 (1989) 234–239.
[10] S. Kawanishi, S. Inoue, K. Yamamoto, Site-specific DNA damage induced by nickel(II) ion in the presence of hydrogen peroxide, Carcinogenesis 10 (1989) 2231–2235.
[11] S. Inoue, S. Kawanishi, ESR evidence for superoxide, hydroxyl radicals and singlet oxygen produced from hydrogen peroxide and nickel(II) complex of glycylglycyl-L-histidine, Biochem. Biophys. Res. Commun. 159 (1989) 445–451.
[12] A. Habib, M. Tabata, Oxidative DNA damage induced by HEPES (2-[4-(2-hydroxyethyl)-1-piperazinyl]ethanesulfonic acid) buffer in the presence of Au(III), J. Inorg. Biochem. 98 (2004) 1696–1702.
[13] J.T. Wu, Y. Huang, J.Z. Zhou, J.Z. Lua, Z.H. Lin, Electrochemical behaviors of DNA at mercury film electrode, Bioelectrochem. Bioenerg. 44 (2004) 151–154.
[14] F. Jelen, M. Fojta, E. Palecek, Voltammetry of native double-stranded, denatured and degraded DNAs, J. Electroanal. Chem. 427 (1997) 49–56.
[15] Z. Wang, D. Liu, S. Dong, In-situ FTIR study on adsorption and oxidation of native and thermally denatured calf thymus DNA at glassy carbon electrodes, Biophys. Chemist. 89 (2001) 87–94.
[16] L. Trnkova, Electrochemical behavior of DNA at a silver electrode studied by cyclic and elimination voltammetry, Talanta 56 (2002) 887–894.
[17] O. Chailapakul, N. Wangfuengkanagul, Electrochemical analysis of -penicillamine using a boron-doped diamond thin film electrode applied to flow injection system, Talanta 58 (2002) 1213.